

# Effect of the ISO 6336-3:2019 Standard Update on the Specified Load Carrying Capacity Against Tooth Root Breakage of Involute Gears

Stefan Sendlbeck, Maximilian Fromberger, Michael Otto, and Karsten Stahl  
Gear Research Center (FZG), Technical University of Munich

## Nomenclature

$C_a$  Tip relief,  $\mu\text{m}$ ;  
 $d_a$  Tip diameter, mm;  
 $d_f$  Root diameter, mm;  
 $d_{Na}$  Active tip diameter, mm;  
 $F_{bt}$  (Nominal) Transverse load in the plane of action (base tangent plane), N;  
 $f_\varepsilon$  Load distribution influence factor;  
 $h^*$  Tool addendum factor;  
 $h_{rc}$  Bending moment lever arm for tooth root stress relevant to load application at the outer point of single pair tooth contact, mm;  
 $h^*$  Tool dedendum factor;  
 $K_A$  Application factor;  
 $m_n$  Normal module, mm;  
 $N_L$  Number of load cycles;  
 $q_t$  Material allowance for finish machining, mm;  
 $S_F$  Safety factor against tooth root breakage;  
 $s_{Fn}$  Tooth root chord at the critical section, mm;  
 $x^*$  Profile shift factor;  
 $Y_F$  Form factor;  
 $Y_\beta$  Helix angle factor;  
 $z_0$  Number of teeth of the tool;  
 $\alpha_{Fen}$  Load direction angle, relevant to direction of application of load at the outer point of single pair tooth contact of virtual spur gears,  $^\circ$ ;  
 $\alpha_n$  Normal pressure angle,  $^\circ$ ;  
 $\alpha_{n0}$  Tool normal pressure angle,  $^\circ$ ;  
 $\alpha_{pr0}$  Tool protuberance angle,  $^\circ$ ;  
 $\beta_b$  Base helix angle,  $^\circ$ ;  
 $\varepsilon_\alpha$  Transverse contact ratio;  
 $\varepsilon_{an}$  Virtual contact ratio of the virtual spur gear;  
 $\varepsilon_\beta$  Overlap ratio;  
 $\theta_{oil}$  Oil temperature,  $^\circ\text{C}$ ;  
 $\rho^*$  Tool tip radius factor;  
 $\rho_{a0}$  Tool tip radius, mm;  
 $\rho_F$  Tooth root radius at the critical section, mm;  
 1 Index for pinion;  
 2 Index for gear wheel;  
 $a$  Center distance, mm;  
 $b$  Face width, mm;  
 $d$  Reference cylinder diameter, mm;  
 LOA Line of action;  
 $n$  Rotational speed,  $\text{min}^{-1}$ ;  
 $pr_0$  Protuberance of the tool, mm;  
 $r$  Relative change of the safety factor against tooth root breakage (2006/2019);  
 $T$  Torque, Nm;  
 $u$  Teeth ratio;  
 $z$  Number of teeth;  
 $\beta$  Reference helix angle,  $^\circ$ .

## Introduction

The ISO 6336 series of standards contains a verified specification for calculating the strength of involute gears. Updates issued in November 2019 contain more detailed calculation methods based on the latest research findings.

Of particular interest here is Part 3 (Ref. 1), which focuses on the tooth bending strength of spur and helical gears and provides a safety factor against tooth root breakage. Following the update of the previous 2006 version (Ref. 2), the revised standard from 2019 (Ref. 1) can yield a higher or lower safety factor depending on the specific gear design. Consequently, to enable an optimal gear design, the gear engineer needs to be aware of the effects of the changes in the standard on the overall result of the calculation.

Therefore, we summarize the current structure of the ISO 6336 standard in this paper and present a detailed review of the key changes introduced in ISO 6336-3:2019 (Ref. 1). We outline the overall effects of the changes in the form of a calculation-based study of different variants with regard to contact ratio and tooth root geometry and compare the results to the ISO 6336-3:2006 (Ref. 2) version.

## Overview of the Current ISO 6336 Structure

The current ISO 6336 series of standards consists of multiple parts that are grouped in international standards, technical specifications and technical reports.

### International standards (ISO 6336):

- Part 1: Basic principles, introduction and general influence factors (Ref. 3)
- Part 2: Calculation of surface durability (pitting) (Ref. 4)
- Part 3: Calculation of tooth bending strength (Ref. 1)
- Part 5: Strength and quality of materials (Ref. 5)
- Part 6: Calculation of service life under variable load (Ref. 6)

### Technical specifications (ISO/TS 6336):

- Part 4: Calculation of tooth flank fracture load capacity (Ref. 7)
- Part 20: Calculation of scuffing load capacity (also applicable to bevel and hypoid gears) — Flash temperature method (Ref. 8)
- Part 21: Calculation of scuffing load capacity (also applicable to bevel and hypoid gears) — Integral temperature method (Ref. 9)
- Part 22: Calculation of micropitting load capacity (Ref. 10)

Additional technical reports (ISO/TR 6336) (Refs. 11–12) containing calculation examples for Part 1, 2, 3, 5 and of micropitting load capacity.

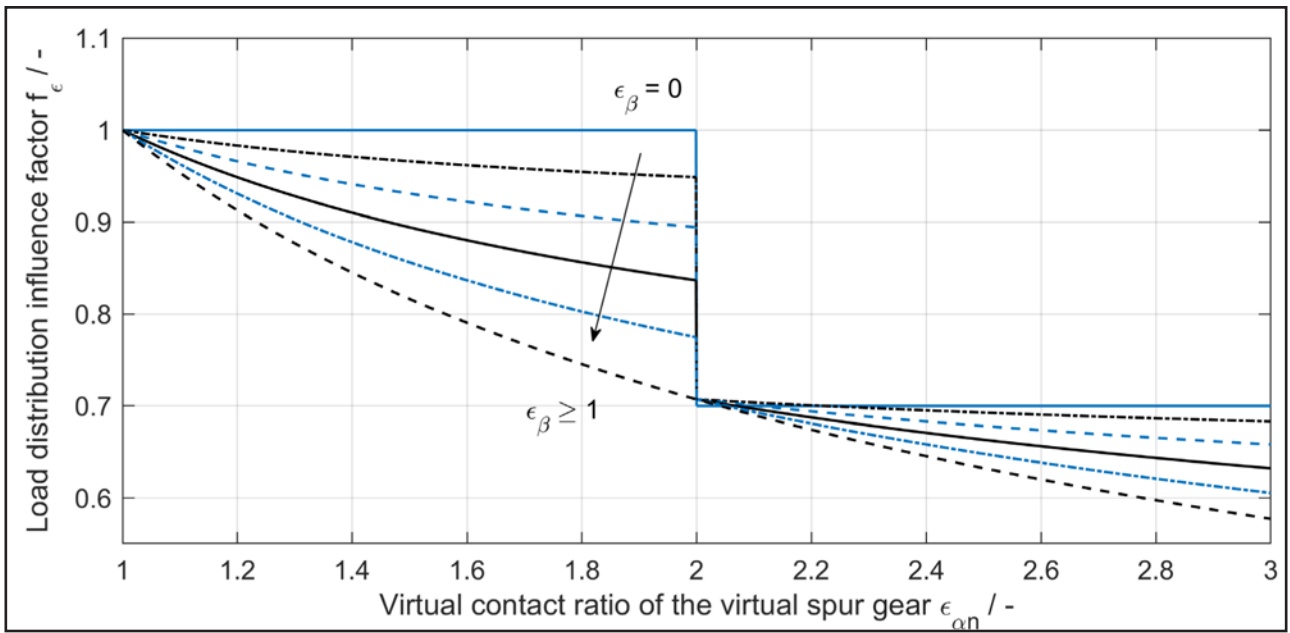


Figure 1 Load distribution influence factor according to ISO 6336-3:2019 (Ref. 1).

### ISO 6336-3:2019 Standard Updates

The revised ISO 6336-3:2019 (Ref. 1) standard contains fundamental changes (i.e., a new load distribution influence factor that accounts for the effects of high overlap ratios and a more precise consideration of the helix angle on the stresses). The determination of the tooth root geometry of internal gears by means of a shaper cutter has also been added to the standard.

### Load Distribution Influence

Load distribution influences affect the tooth root stresses of gears, they are crucial for calculating the bending strength of the gears, and are therefore an ongoing field of research (Refs. 13–15). Gears and especially helical gears with high contact ratios proved to normally have a higher bending strength than predicted with previous ISO 6336-3:2006 (Ref. 2) calculations (Refs. 16–17).

According to the ISO 6336-3 specification, the location for determining the nominal tooth root stress is in the tooth root area at the 30°/60° tangent to the center line for external/internal gears, respectively (see Fig. 2). The calculation variables derived at this critical section are the bending moment lever arm  $h_{Fe}$ , the tooth root chord  $s_{Fn}$ , and the tooth root radius  $\rho_F$ . Based on this, the form factor  $Y_F$  accounts for influences of the tooth shape on the tooth root stresses with a load applied at the outer point of the single pair tooth contact.

In the current ISO 6336-3:2019 (Ref. 1) standard, the new load distribution influence factor  $f_\epsilon$  extends the previous calculation of the form factor  $Y_F$  from ISO 6336-3:2006 (Ref. 2) (see Eq. 1). It accounts for stress-reducing effects by applying a more favorable load distribution over several pairs of teeth for deep teeth at high contact ratios (Refs. 16,18). The load distribution influence factor is  $f_\epsilon \leq 1$ .

$$Y_F = \frac{6h_{Fe} \cos \alpha_{Fen}}{m_n \left(\frac{s_{Fn}}{m_n}\right)^2 \cos \alpha_n} \cdot f_\epsilon \quad (1)$$

where

$Y_F$  is the form factor

$h_{Fe}$  is the bending moment lever arm for tooth root stress relevant to load application at the outer point of single pair tooth contact, mm;

$m_n$  is the normal module, mm;

$s_{Fn}$  is the tooth root chord at the critical section, mm;

$\alpha_{Fen}$  is the load direction angle, relevant to the direction of application of load at the outer point of single pair tooth contact of virtual spur gears, °;

$\alpha_n$  is the normal pressure angle, °;

$f_\epsilon$  is the load distribution influence factor.

For a load distribution influence factor of  $f_\epsilon = 1$ , there is no change in the ISO 6336-3:2019 (Ref. 1) calculation compared to the previous version, ISO 6336-3:2006 (Ref. 2). However, when the load distribution influence factor is  $f_\epsilon < 1$ , the different versions vary, resulting in a reduced form factor  $Y_F$  in ISO 6336-3:2019 (Ref. 1), which, in turn, causes a smaller calculated tooth root stress.

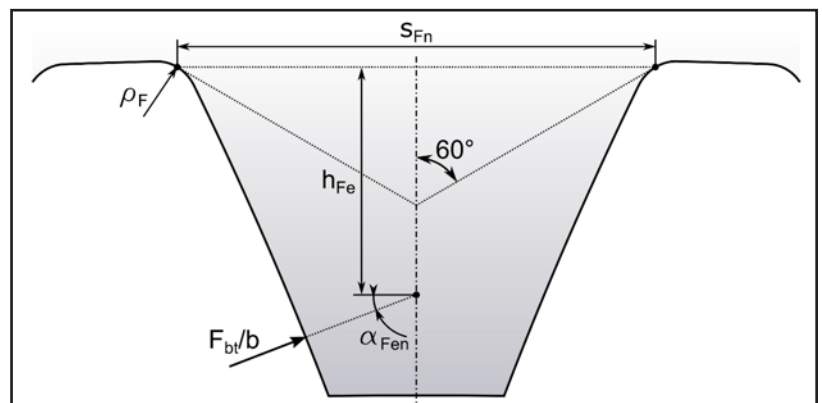


Figure 2 Geometrical variables at the critical section for internal gears according to ISO 6336-3:2019 (Ref. 1).

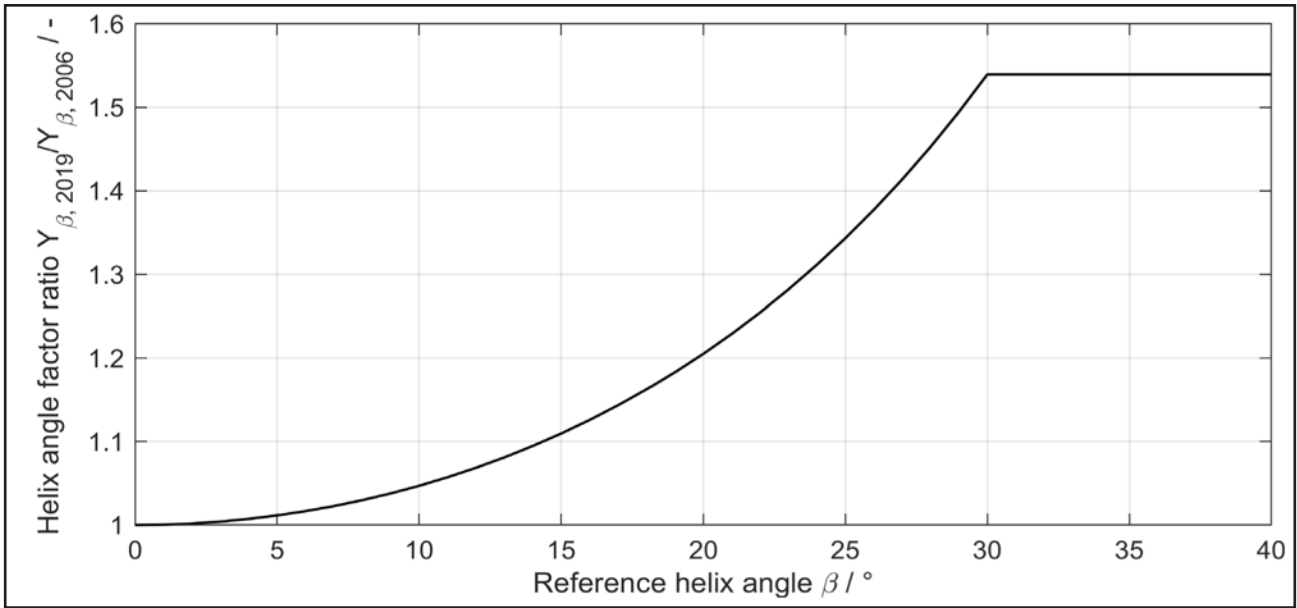


Figure 3 Helix angle factor ratio of ISO 6336-3:2019 (Ref. 1) and ISO 6336-3:2006 (Ref. 2).

In detail, the load distribution influence factor  $f_\varepsilon$  depends on the contact ratio of the spur gear  $\varepsilon_\alpha$  or the virtual contact ratio of the virtual spur gear  $\varepsilon_{an}$  and the overlap ratio  $\varepsilon_\beta$  (see Eqs. 2–7). An overview is given in Figure 1.

For spur gears with a transverse contact ratio of  $\varepsilon_\alpha \geq 2$  the new load distribution influence factor produces a smaller form factor and, in turn, a lower calculated stress in the tooth root according to Equation 2 and Equation 3.

$$f_\varepsilon = 1.0 \quad \text{for } \varepsilon_\beta = 0, \varepsilon_\alpha < 2 \quad (2)$$

$$f_\varepsilon = 0.7 \quad \text{for } \varepsilon_\beta = 0, \varepsilon_\alpha \geq 2 \quad (3)$$

where

$f_\varepsilon$  is the load distribution influence factor;

$\varepsilon_\alpha$  is the transverse contact ratio;

$\varepsilon_\beta$  is the overlap ratio.

For helical gears, an equivalent virtual spur gear forms the basis of the calculation. The virtual contact ratio  $\varepsilon_{an}$  results from the transverse contact ratio  $\varepsilon_\alpha$  of the helical gear and its base helix angle  $\beta_b$  according to Equation 4.

$$\varepsilon_{an} = \frac{\varepsilon_\alpha}{\cos^2 \beta_b} \quad (4)$$

where

$\varepsilon_{an}$  is the virtual contact ratio of the virtual spur gear;

$\varepsilon_\alpha$  is the transverse contact ratio;

$\beta_b$  is the base helix angle,  $^\circ$ .

The new load distribution influence factor for helical gears according to Equations 5–7 tends to lower both the form factor and the calculated tooth root stress as the virtual transverse contact ratio  $\varepsilon_{an}$  and overlap ratio  $\varepsilon_\beta$  increase.

$$f_\varepsilon = \varepsilon_{an}^{0.5} \quad \text{for } \varepsilon_\beta \geq 1 \quad (5)$$

$$f_\varepsilon = \left(1 - \varepsilon_\beta + \frac{\varepsilon_\beta}{\varepsilon_{an}}\right)^{0.5} \quad \text{for } 0 < \varepsilon_\beta < 1, \varepsilon_{an} < 2 \quad (6)$$

$$f_\varepsilon = \left(\frac{1 - \varepsilon_\beta}{2} + \frac{\varepsilon_\beta}{\varepsilon_{an}}\right)^{0.5} \quad \text{for } 0 < \varepsilon_\beta < 1, \varepsilon_{an} \geq 2 \quad (7)$$

where

$f_\varepsilon$  is the load distribution influence factor;

$\varepsilon_{an}$  is the virtual contact ratio of the virtual spur gear;

$\varepsilon_\beta$  is the overlap ratio.

### Determining the Tooth Root Geometry

Bending moment lever arm  $h_{Fe}$ , tooth root chord  $s_{Fm}$ , and tooth root radius  $\rho_F$  are the variables at the critical section that are key to calculating the form factor  $Y_F$  with Equation 1, and they account for the influence of the tooth and, in particular, the root shape on the maximum calculated nominal tooth root stress from ISO 6336-3. The necessary geometrical properties are illustrated in Figure 2, with the load applied at the outer point of the single pair tooth contact (face width specific transverse load in the plane of action  $F_{bt}/b$ , load direction angle  $\alpha_{Fen}$ ).

For external gears, no fundamental changes apply, and ISO 6336-3:2019 (Ref. 1) follows ISO 6336-3:2006 (Ref. 2) in quantizing the geometrical variables relevant to the tooth root stress calculation illustrated in Figure 2. The geometrical variables are determined according to the manufacturing principle of using toothed rack-like tools, such as gear hobs.

For internal gears, ISO 6336-3:2019 (Ref. 1) presents a modified method of calculating the following three geometrical variables at the critical section: bending moment lever arm  $h_{Fe}$ , tooth root chord  $s_{Fm}$ , and tooth root radius  $\rho_F$ . Theoretical and experimental research have shown that determining the tooth root geometry of internal gears based on the tool roll-off of a shaper cutter yields a more precise basis for tooth root stress and bending strength calculation (Refs. 19–21).

The previous version of ISO 6336-3:2006 (Ref. 2) uses a simplified calculation method to determine the form factor variables. This calculation is based on the principle that internal gearing is manufactured using a virtual toothed rack-like tool. The method thus follows the calculation of external gears with a toothed rack-like tool.

In ISO 6336-3:2019 (Ref. 1), however, the principle used for internal gearing calculation is that gears are made with a shaper cutter and its associated roll-off, in accordance with VDI 2737:2016 (Ref. 21) guideline. The shape of the tool corresponds to a pinion conjugate to the internal teeth of the ring gear. As with external gears produced with a toothed rack-like tool, the contour of the tooth root is defined by the relative path of the

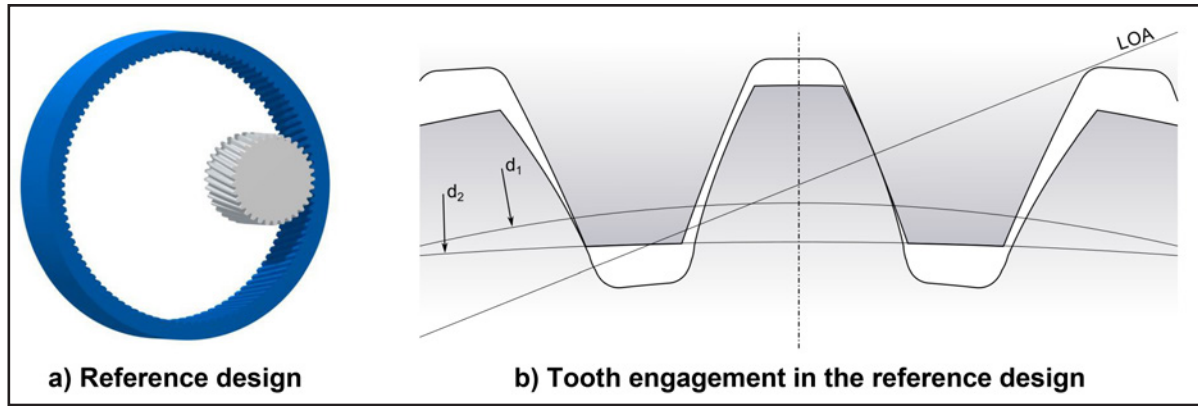


Figure 4 Reference design and tooth engagement in the external-internal gear stage.

tool boundary and therefore allows the geometrical variables of the form factor of internal gears to be determined directly, based on the tool contour.

### Influence of the Helix Angle

The helix angle factor  $Y_\beta$  is part of the ISO 6336-3 calculation for adjusting the calculated tooth root stress of the virtual spur gear to the actual tooth root stress of the helical gear; the influence of the helix angle is thus accounted for.

In ISO 6336-3:2006 (Ref. 2), the helix angle factor is determined by Equation 8. If  $\beta$  would exceed  $30^\circ$ ,  $\beta$  remains constant at  $\beta = 30^\circ$  when calculating the helix angle factor.

$$Y_\beta = 1 - \varepsilon_\beta \frac{\beta}{120^\circ} \quad (8)$$

where

$Y_\beta$  is the helix angle factor;  
 $\beta$  is the reference helix angle,  $^\circ$ ;  
 $\varepsilon_\beta$  is the overlap ratio.

Many experiments for determining the tooth root strength are done with spur gears. Additional research findings based on helical gear experiments and advanced calculations show that slightly modifying the helix angle factor depending on the helix angle would better represent the helix angle influence and therefore would lead to a more accurate stress calculation (Refs. 16–17).

Following the update in accordance with the research findings, Equation 9 applies to ISO 6336-3:2019 (Ref. 1). If  $\beta$  would exceed  $30^\circ$ ,  $\beta$  remains constant at  $\beta = 30^\circ$  when calculating the helix angle factor.

$$Y_\beta = \left(1 - \varepsilon_\beta \frac{\beta}{120^\circ}\right) \frac{1}{\cos^3 \beta} \quad (9)$$

where

$Y_\beta$  is the helix angle factor;  
 $\beta$  is the reference helix angle,  $^\circ$ ;  
 $\varepsilon_\beta$  is the overlap ratio.

Taking into account Equations 8 and 9, Equation 10 represents the effective change resulting from ISO 6336-3:2019 (Ref. 1) compared to ISO 6336-3:2006 (Ref. 2) owing to the helix angle factor ratio of  $Y_{\beta,2019}/Y_{\beta,2006}$ . It is additionally illustrated in Figure 3.

$$Y_{\beta,2019}/Y_{\beta,2006} = \frac{1}{\cos^3 \beta} \quad (10)$$

where

$Y_\beta$  is the helix angle factor;  
 $\beta$  is the reference helix angle,  $^\circ$ .

### Calculation Study

To investigate the overall effects of these changes, we varied the contact ratio by using gears with different transverse contact ratios and different overlap ratios as a basis for computing the specifications of the standard. By simultaneously varying the transmission ratio and the tool tip radius, we investigated the effect of different internal-gear tooth-root geometries on the calculation.

To enable the calculation study of variants, first, a reference gear design was defined that is as close as possible to one used in everyday practice. We then varied selected gear geometry parameters while keeping the face load and the load influence factors constant. This enabled us to keep general load influences separate from solely geometric changes and to investigate the effects of the changes between the ISO 6336-3:2006 (Ref. 2) and the ISO 6336-3:2019 (Ref. 1) standards selectively.

The reference gear design used is a helical external-internal gear stage with a case-hardened pinion and a hardened and tempered wheel (see Fig. 4 and Tables 1–4). The tip diameter and

Table 1 Reference design – fundamental data		
	Pinion	Ring gear
Number of teeth $z$	33	–103
Tip diameter $d_a$	107.50 mm	–313.74 mm
Root diameter $d_f$	96.09 mm	–324.63 mm
Center distance $a$	–107.78 mm	
Normal module $m_n$	3.00 mm	
Normal pressure angle $\alpha_n$	20.00 $^\circ$	
Face width $b$	80.00 mm	
Profile shift factor $x^*$	0.40	–0.80
Transverse contact ratio $\varepsilon_\alpha$	1.23	
Overlap ratio $\varepsilon_\beta$	1.47	
Reference helix angle $\beta$	10.00 $^\circ$	
Material	18CrNiMo7-6 case-hardened	42CrMo4 hardened and tempered

Table 2 Reference design – tool data (roughing)		
	Pinion	Ring Gear
Tool	Gear hob	–
Tool normal module $m_n$	3.00 mm	–
Tool normal pressure angle $\alpha_{r0}$	20.00 $^\circ$	–
Tool addendum factor $h_{aP0}^*$	1.30	–
Tool dedendum factor $h_{fP0}^*$	1.80	–
Tool tip radius factor $\rho_{a0}^*$	0.20	–
Protuberance of the tool $\rho_{r0}$	0.30 mm	–
Tool protuberance angle $\alpha_{p0}$	10.00 mm	–
Material allowance for finish machining $q_f$	0.28 mm	–

Table 3 Reference design – tool data (finishing)		
Tool	Pinion	Ring gear
Tool normal module $m_n$	Grinding disc	Shaper cutter
Tool normal pressure angle $\alpha_{rn}$	3.00 mm	
Tool addendum factor $h_{ap0}^*$	20.00°	
Tool dedendum factor $h_{fp0}^*$	1.10	1.00
Tool tip radius factor $\rho_{a0}^*$	1.80	1.77
Number of teeth of the tool $z_0$	0.20	29

Table 4 Reference design – additional data		
	Pinion	Ring gear
Gear tooth quality ISO 1328:2013	5	
Torque $T$	2000 Nm	6242 Nm
Rotational speed $n$	3000 $\frac{1}{\text{min}}$	961 $\frac{1}{\text{min}}$
Number of load cycles $N_L$	171.7 Mio	55.0 Mio
Lubricant	FVA-3A	
Oil temperature $\theta_{oil}$	60°	
Lead correction	-	
Tip relief $C_a$	18 $\mu\text{m}$	
Application factor $K_A$	1.0	

Table 5 Variation range (contact ratio) based on reference design		
Variation		
Torque $T$ and face width $b$	T/b (const.) $\rightarrow \epsilon_\beta = 0.07 \dots 2.21$	
Active tip diameter $d_{Na}$ and tool addendum factor $h_{ap0}^*$	$c^*$ (const.) $\rightarrow \epsilon_\alpha = 1.30 \dots 2.10$	

not the tool dedendum defines the gear tips to ensure that the tool dedendum does not influence the results of the calculation study in the following.

For each variant of the calculation study, we determined the safety factor against tooth root breakage according to the calculation specification in the standard. This allowed us to compare the relative change  $r$  between the two ISO 6336-3 versions as a percentage, using Equation 11 with the safety factor of ISO 6336-3:2006 (Ref. 2) as a reference value.

$$r = S_{F,ISO6336:2006 \rightarrow ISO6336:2019} = \frac{\Delta S_F}{S_F} + \frac{S_{F,ISO6336:2019} - S_{F,ISO6336:2006}}{S_{F,ISO6336:2006}} \tag{11}$$

where

$r$  is the relative change of the safety factor against tooth root breakage (2006/2019)

$S_F$  is the safety factor against tooth root breakage

### Variation in Contact Ratio

In the following, the new load distribution influence factor  $f_\epsilon$  in combination with the modified helix angle factor  $Y_\beta$  as described in Load Distribution Influence (p.45) and Influence of the Helix Angle (p.47) are investigated by varying the contact ratio.

### Variation in Contact Ratio — Method

Starting from the reference design, we simultaneously varied both the transverse contact ratio  $\epsilon_\alpha$  and the overlap ratio  $\epsilon_\beta$  in accordance with Table 5.

Varying the overlap ratio is possible by changing the helix angle  $\beta$  or the face width  $b$ , with a non-zero helix angle assumed. Because the specific face load needs to remain as constant as possible to achieve comparable results, we varied the face width  $b$  and the torque  $T$  so as to keep  $T/b$  constant and thus change the overlap ratio. This is possible because the reference helix angle of the reference design is  $\beta > 0$ . The advantage is that the variation does not cause the gear and root shape to change.

To influence the transverse contact ratio, we changed the active tip diameter  $d_{Na}$  in conjunction with the tool addendum factor  $h_{ap0}^*$ . Although this allows us to keep the relative tip clearance  $c^*$  constant, it results in the tooth root geometries changing within the range of the variation (Fig. 5). It should be noted that another option is a single change in the active tip diameter, which results in gear meshes with different tip clearances and a constant tooth root geometry. But the shapes tend to be highly impractical in everyday applications. It is for this reason that we chose the above approach.

A two-dimensional mesh of 40 linearly distributed calculation points in the transverse contact ratio direction and the overlap ratio direction is the basis for all plots in the following. Each contour plot therefore contains 1,600 calculations of standard comparisons.

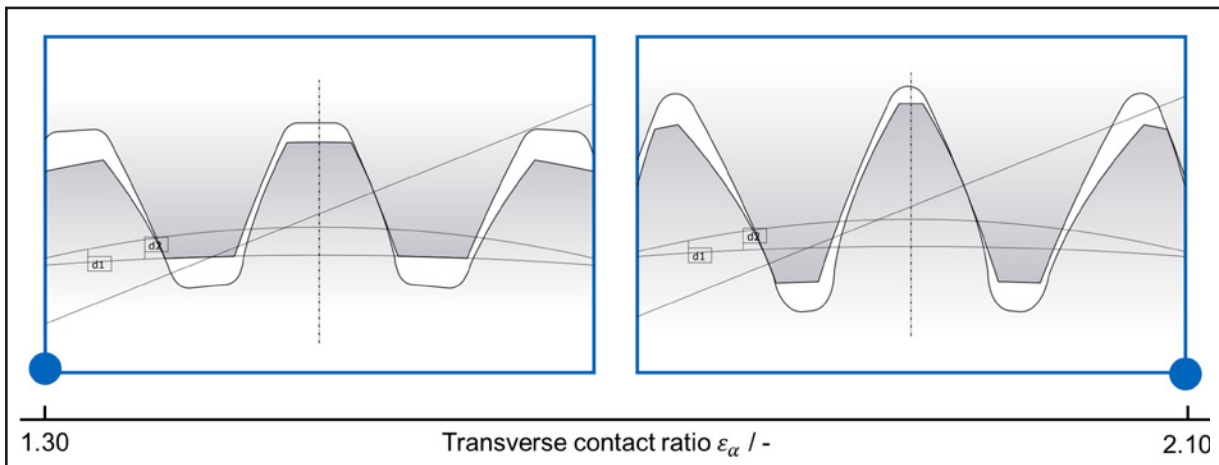


Figure 5 Gear variation with respect to transverse contact ratio.

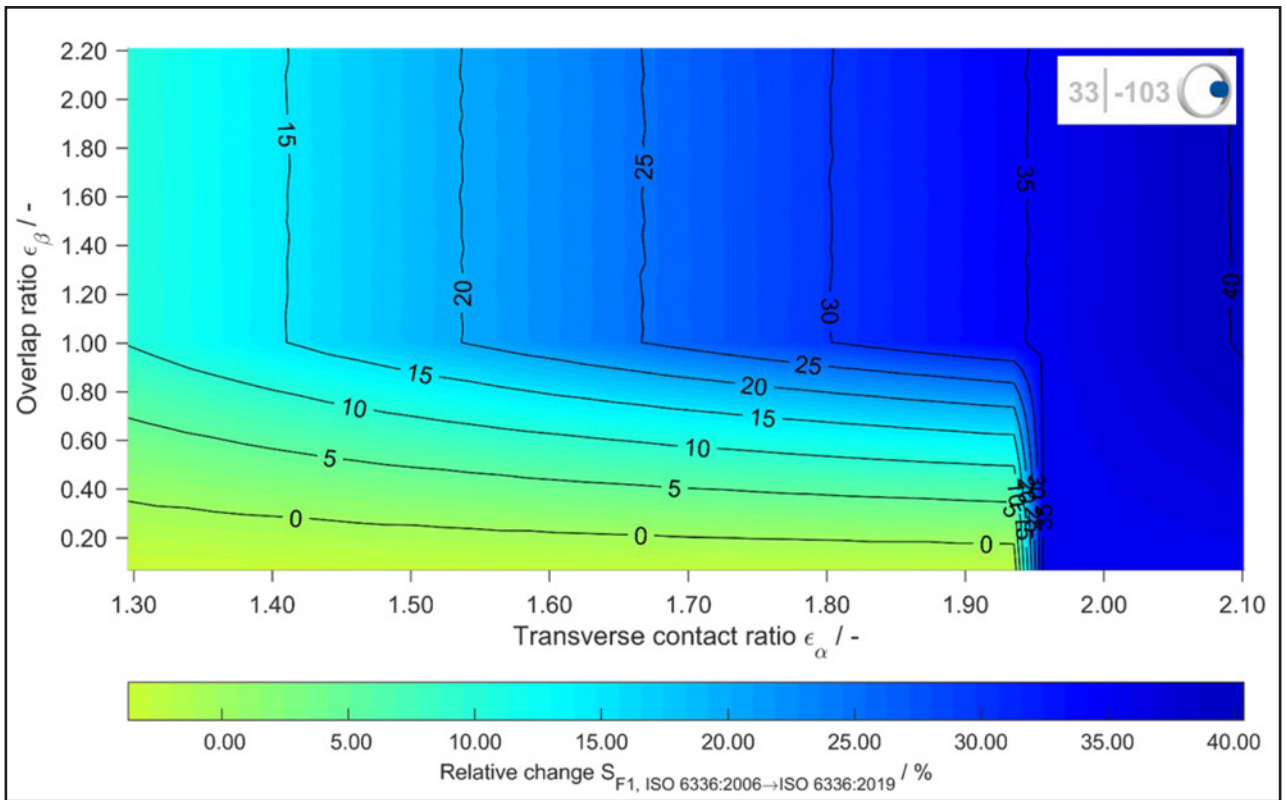


Figure 6 Relative change in the safety factor against tooth root breakage  $S_{F1}$  for the pinion,  $40 \times 40$  calculation points.

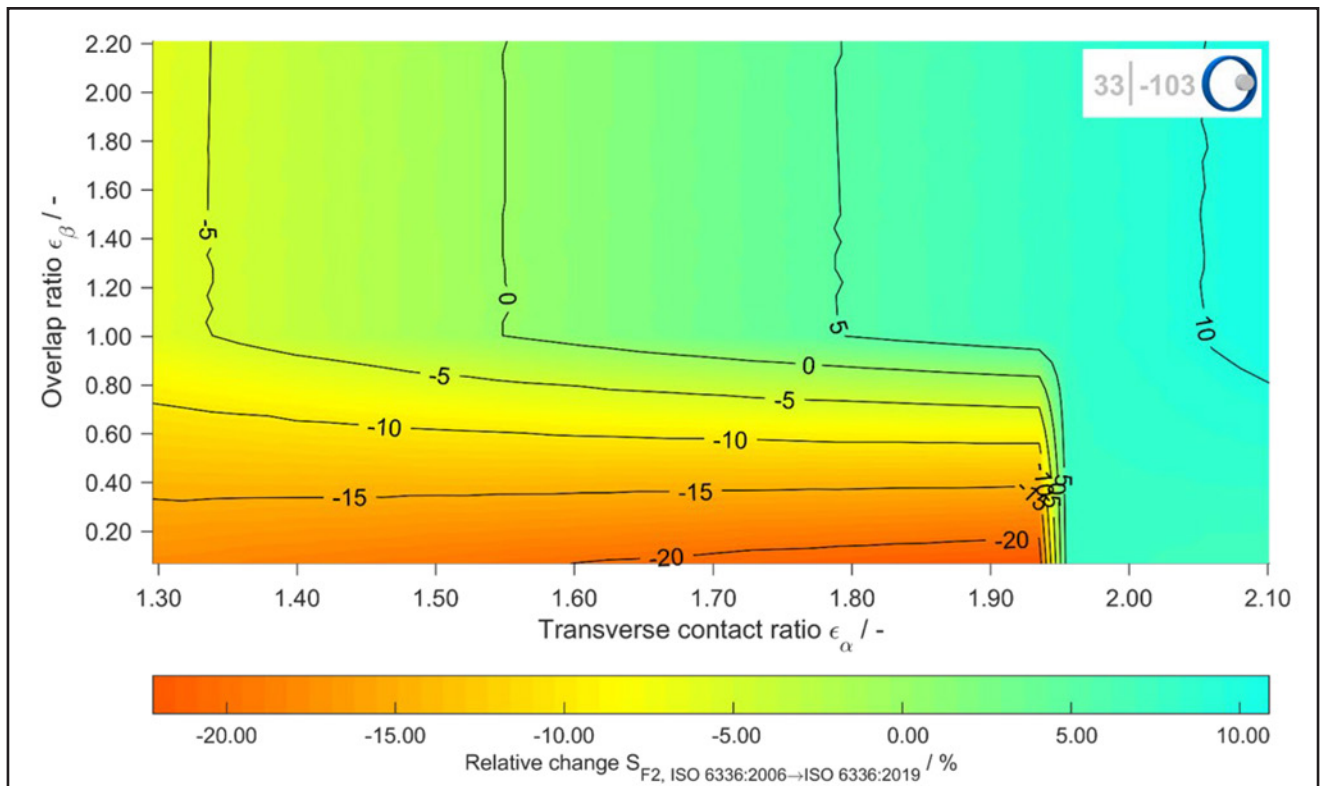


Figure 7 Relative change in the safety factor against tooth root breakage  $S_{F2}$  for the wheel,  $40 \times 40$  calculation points.

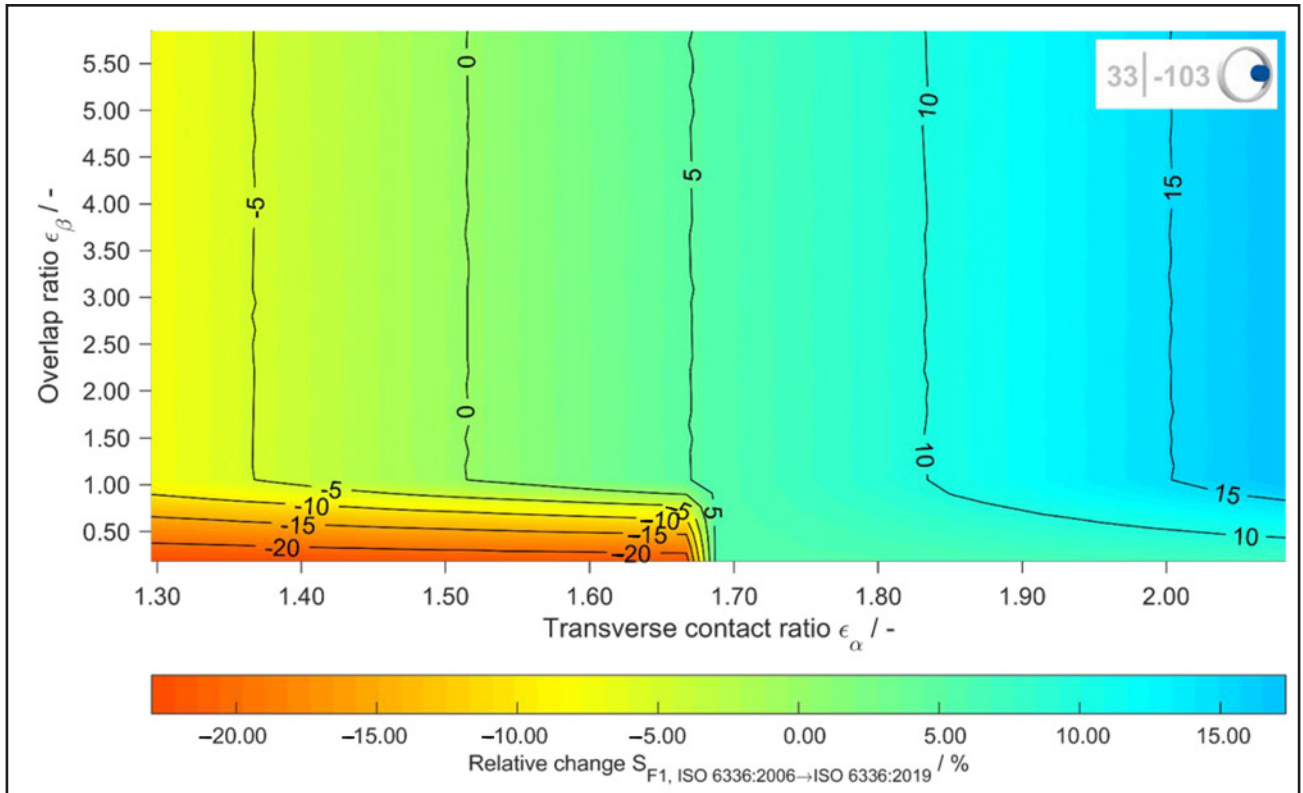


Figure 8 Relative change in the safety factor against tooth root breakage  $S_{F1}$  for the pinion, reference helix angle  $\beta=25^\circ$ ,  $40 \times 40$  calculation points.

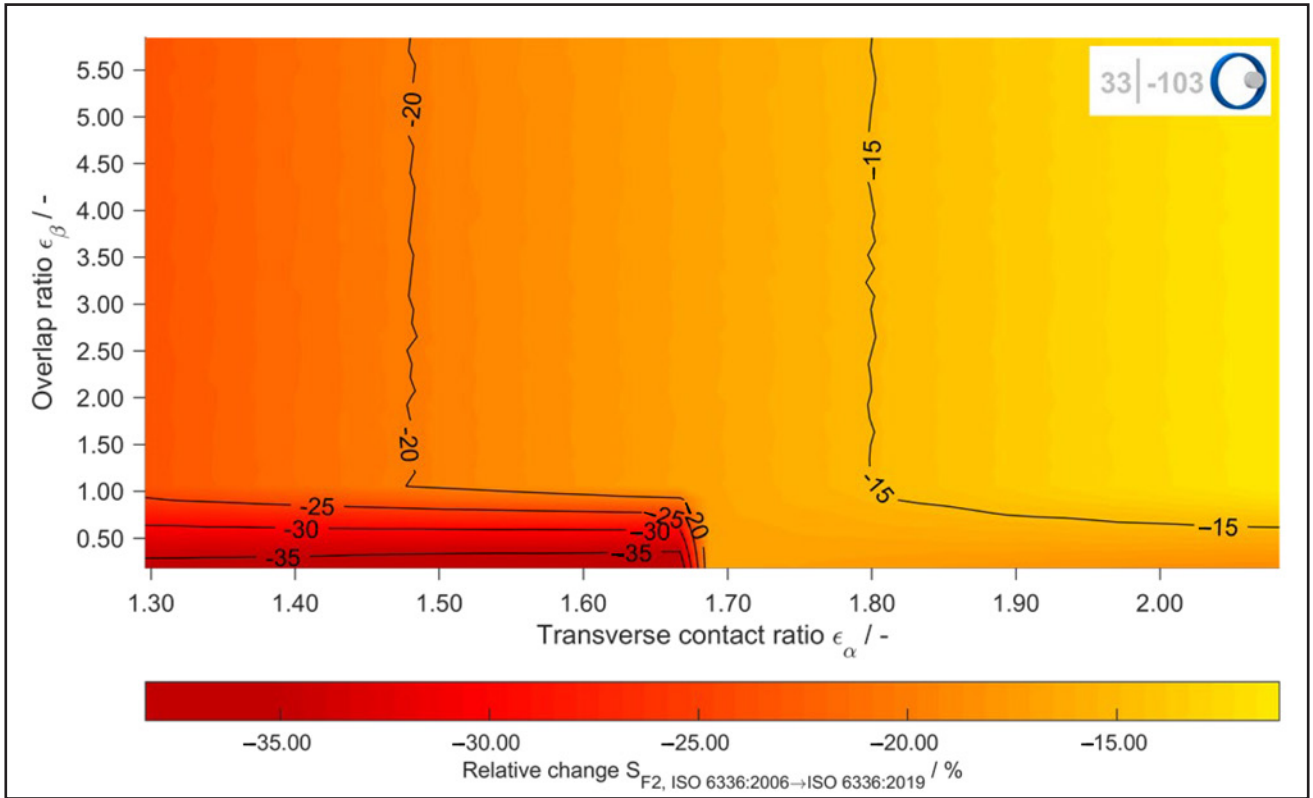


Figure 9 Relative change in the safety factor against tooth root breakage  $S_{F2}$  for the wheel, reference helix angle  $\beta=25^\circ$ ,  $40 \times 40$  calculation points.

## Variation in Contact Ratio — Results

Figure 6 provides the results of the variation calculation of the external gear pinion in external-internal gear pairs according to the procedure described in Variation in Contact Ratio — Method (p.48). The load distribution influence factor  $f_e$  added in the updated standard from 2019 generally leads to an increase in the safety factor against tooth root breakage compared to the 2006 version. The helix angle factor  $Y_\beta$  has only marginal influence on the results. As shown in Figure 3, it reduces the relative change by less than 5%, independently of the contact ratio.

For overlap ratios of  $\varepsilon_\beta \geq 1$ , the safety factor increases almost linearly as the transverse contact ratio increases. The relative change ranges from approximately +10% at a transverse contact ratio of  $\varepsilon_\alpha \approx 1.3$  to approximately +40% at a transverse contact ratio of  $\varepsilon_\alpha \approx 2.1$ .

At a low overlap ratio of  $\varepsilon_\beta \approx 0$ , the data in the diagram displays a distinct step at a transverse contact ratio of  $\varepsilon_\alpha \approx 1.95$ . According to the determination of the load distribution influence factor  $f_e$  a step should occur for spur gears when the virtual contact ratio of the virtual spur gear  $\varepsilon_{\alpha n} = 2.0$ . This is valid when applying the relation between helical gears and virtual spur gears described by Equation 4. In the overlap ratio range of  $0 < \varepsilon_\beta < 1$ , the relative change in the safety factor increases continuously from low to high.

The results for the internal gear wheel are shown in Figure 7. As with the external gear pinion shown in Figure 6, the characteristic influence of the load distribution influence factor is present, but the relative change in the safety factor against tooth root breakage is smaller. While the load distribution influence factor tends to lead to a higher safety factor, changes are additionally caused by the modified calculation of the tooth root geometry for internal gears according to Determining the Tooth Root Geometry (p.46). As a result, the relative change in the safety factor varies from approximately -20% to +10%, depending on the transverse contact ratio and the overlap ratio.

The calculation study also covers variations in the helix angle. While the reference design has a reference helix angle of  $\beta = 10^\circ$  and the changes in the helix angle factor are thus of relatively low impact, the results shown in Figure 8 and Figure 9 are based on a reference helix angle of  $\beta = 25^\circ$  for pinion and wheel, respectively. To enable comparability of the results, we also changed the normal module  $m_n$ , the normal pressure angle  $\alpha_n$  and the profile shift factors beside the helix angle with respect to the reference design such that the gear teeth in the transverse plane corresponded as closely as possible within the variation range.

In areas of low transverse contact ratios  $\varepsilon_\alpha$  and especially with additionally low overlap ratios  $\varepsilon_\beta$ , the calculation according to the new ISO 6336-3:2019 (Ref. 1) results in a lower safety factor against tooth root breakage than the previous version. It increases with higher transverse contact ratios. Due to the higher reference helix angle compared to the reference design, the step in the relative change in the safety factor against tooth root breakage at low overlap ratios shifts to a lower transverse contact ratio of  $\varepsilon_\alpha \approx 1.68$ . This is the effect of a high helix angle and the associated relation between the transverse contact ratio of helical gears and its virtual spur gear (Eq. 4).

The generally lower values of the relative change in the safety factors against tooth root breakage compared with previous investigations shown in Figure 6 and Figure 7 are a result of the change in the helix angle factor  $Y_\beta$ . The load distribution influence factor  $f_e$  tends to have a stress-reducing effect, which leads to an increase in the safety factor. However, with increasing helix angle, the modified calculation of the helix angle factor shows a greater and greater impact in accordance with the relations illustrated in Figure 3. This generally causes an increase in calculated stresses and, consequently, a reduced safety factor against tooth root breakage. Thus, the helix angle factor counteracts the effects of the load distribution influence factor, especially at high helix angles.

## Variation in Tooth Root Geometry

Due to the new specification for calculating geometric gear properties, the tooth root geometry and its impact on the safety factor against tooth root breakage presented in Determining the Tooth Root Geometry (p.48) are also investigated. The focus is on internal gears and their tooth root, since it is these that are affected by the revised standard, as the root geometry is now additionally determined using a shaper cutter tool.

## Variation in Tooth Root Geometry — Method

To investigate the influences of the changes such that the tooth root geometry is determined in ISO 6336-3:2019 (Ref. 6), we examined several tooth root geometries of internal-external gears. Starting from the reference design, we simultaneously varied the teeth ratio  $|u|$ , thus the transmission ratio, and the tooth root fillet by adapting the tip radius of the tool  $\rho_{a0}$  (see Table 6).

Table 6 Variation range (tooth root geometry) based on reference design	
Variation	
Number of teeth of the wheel $z_2$	$z_1 = 33$ (const.); $z_2 = -115 \dots -60$
Tool tip radius factor $\rho_{a0}^*$	$\rho_{a0}^* = 0.10 \dots 0.38$

The teeth ratio  $|u|$  is varied by changing the number of teeth of the wheel  $z_2$  within a wide range while keeping the number of teeth of the pinion  $z_1$  constant (Fig. 10).

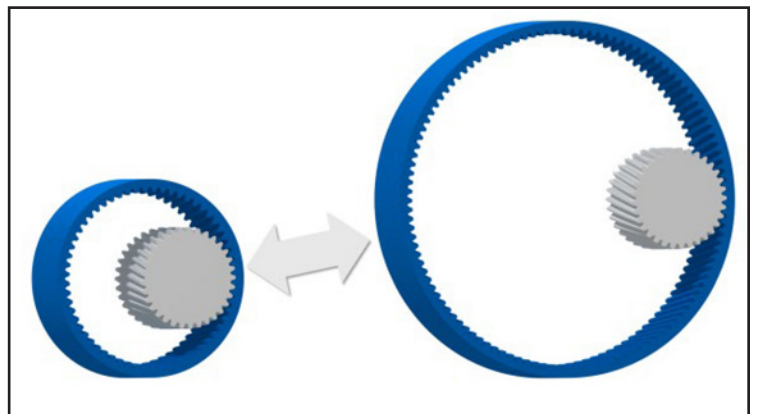


Figure 10 Variation in tooth root geometry and transmission ratio/teeth ratio.

To ensure comparability of the results, the transverse contact ratio  $\varepsilon_\alpha$  and overlap ratio  $\varepsilon_\beta$  should be kept constant throughout this variation. The overlap ratio depends on the helix angle

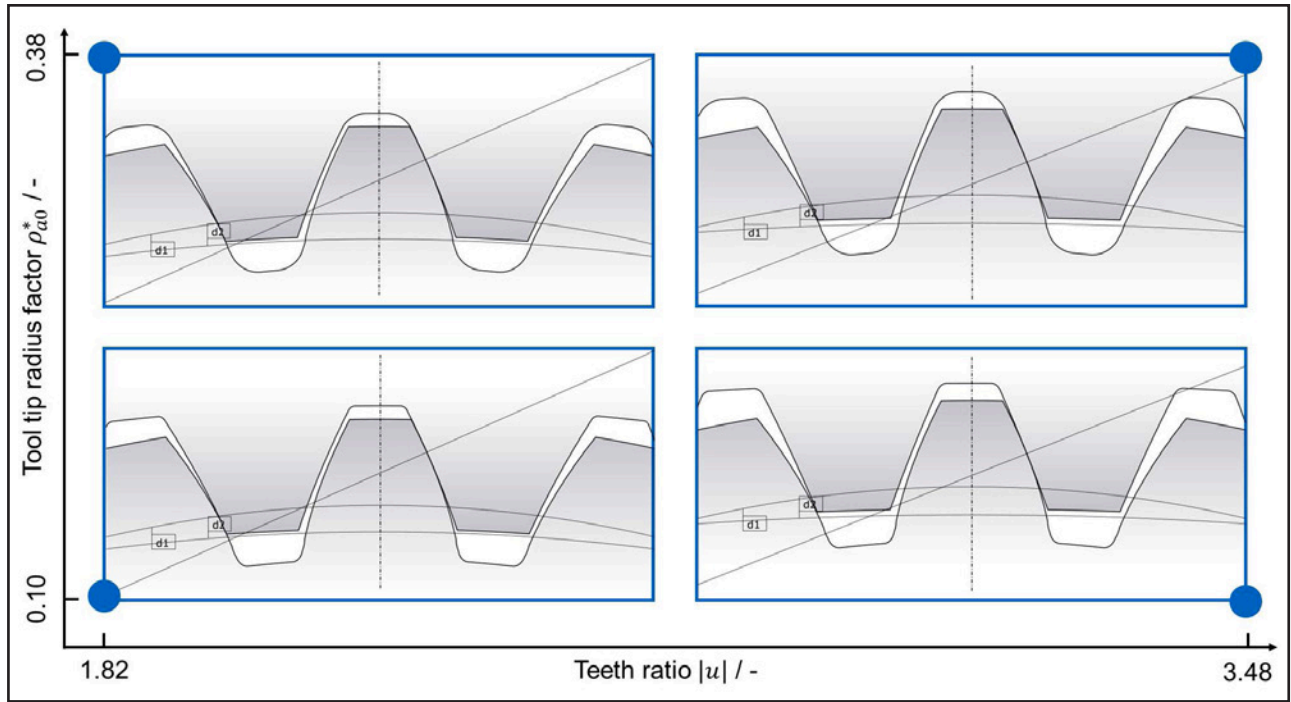


Figure 11 Gear variation with respect to teeth ratio and tool tip radius factor.

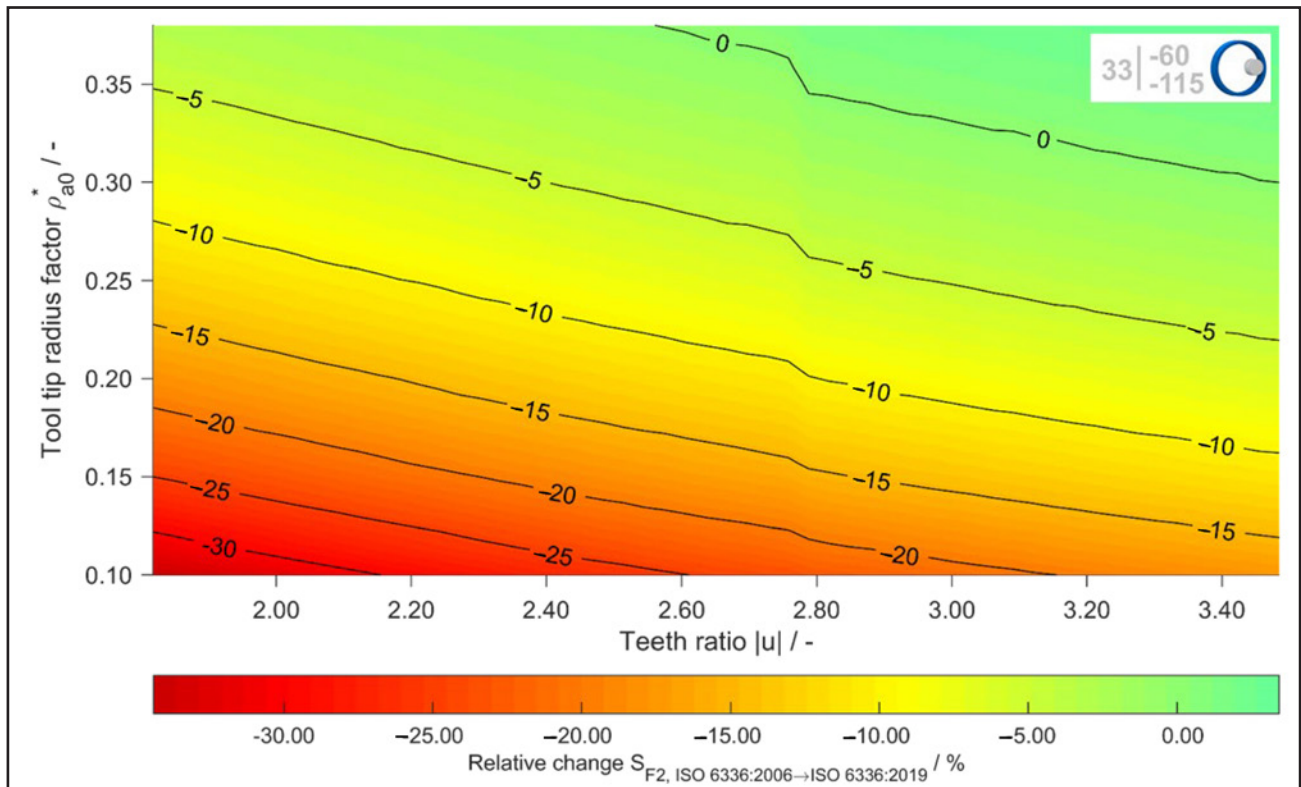


Figure 12 Relative change in the safety factor against tooth root breakage  $S_{F2}$  for the wheel,  $56 \times 40$  calculation points.

and the face width of the gear. Because both parameters are constant while the tooth root geometry is varied, the overlap ratio does not change. However, the transverse contact ratio can change as a result of the changing transmission ratio. With the same module and tools, the center distance  $a$  increases as the number of teeth of the wheel increases. As a result, both the reference diameter and tip diameter also increase. As the tip diameter  $d_{Na} = d_a$  is predefined and is not a tool-dependent variable, changing the tip diameter within a certain range allows the transverse contact ratio to be influenced for each variant of the internal gear. We therefore conduct one-dimensional optimization by varying the tip diameter to keep the transverse contact ratio constant independently of the number of teeth of the wheel and, in turn, independently of the transmission ratio.

Additionally, the curvature of the tooth root fillet ranges from minimal to fully rounded. In this case, the variation is based on the tool tip radius factor  $\rho^*$ .

The boundary gear mesh geometries in the transverse section of the calculation study, used to investigate the tooth root influence, are shown in Figure 11.

A two-dimensional mesh of 40 linearly distributed calculation points in the tool tip radius factor direction and 56 in the teeth ratio direction is the basis for the plot in the following. The contour plot therefore contains 2,240 calculations of standard comparisons.

## Variation in Tooth Root Geometry — Results

Figure 12 provides the results of the calculation study in terms of tooth root geometry influences as described in Variation in Tooth Root Geometry — Method (p.51) for the internal gear.

There are only small deviations in the safety factor against tooth root breakage between ISO 6336-3:2019 (Ref. 1) and the 2006 version; these are in the range of high teeth ratios with a large tool tip radius. As the teeth ratio and the tooth root fillet curvature become smaller, the relative change in the safety factor decreases. Thus, ISO 6336-3:2019 (Ref. 1) shows lower safety values against tooth root breakage than the previous version for a range of gear geometries. It is worth mentioning that the results presented in Figure 12 include an almost constant offset of +7.81%, due to the impact of the updated helix angle factor  $Y_\beta$  and the newly added load distribution influence factor  $f_s$ .

The results shown in Figure 12 are based on the updated method of calculating the geometrical properties of the bending moment lever arm  $h_{Fe}$ , the tooth root chord  $s_{Fn}$ , and the tooth root radius  $\rho_F$  at the critical section. The calculated bending moment lever arm according to ISO 6336-3:2019 (Ref. 1) is approximately -8.5% to -12.0% lower than in the previous version and almost independent of the tooth root fillet curvature. The updated standard did not result in any appreciable change to the tooth root chord. The relative change is within a range of -2.0% to 0.0%. However, the tooth root radius at the critical section changed gradually from high teeth ratios and tool tip radii, with relative changes from approximately -20.0% to -70.0% towards lower values.

The updated standard did not result in any changes to the calculation of the tooth root geometry for external gears and so there is no change to the resulting safety against tooth root breakage.

## Discussion

We chose the reference design and the variants derived from such as to cover a wide range of influences on the calculation given in the new standard; however, the calculation study does not cover every possible gear geometry and constellation. Nonetheless, the results of the calculation study give a broad insight into the updated standard and enables the engineer to assess its overall effects. To improve the comparability of the results, we limited the variation to a few key parameters, even if varying several parameters at a time would have helped remain within a practical range of gears. This compromise makes it easier to isolate the individual changes in the standard and shows their effect on the calculation in the standard as a whole. The inclusion of the root geometry calculation for internal gears in particular enables the engineer to comprehend the direct effects of the updated standard on the safety factor against tooth root breakage.

## Conclusion

This paper provides a compact overview of the main changes in the updated calculation in ISO 6336 Part 3 from 2019 and its effects on the analysis of the tooth-bending strength of involute gears.

The most important changes include a new load distribution influence factor that accounts for the effects of high overlap ratios. An updated version of the helix angle factor refines the influence of the helix angle on the stresses. Additionally, the manufacturing principle of a shaper cutter is now the basis for determining the tooth root geometry for internal gears and has an effect on the relevant geometrical calculation variables, namely the tooth root curvature, the tooth root chord and the associated bending moment lever arm.

By varying both the transverse contact ratio and the overlap ratio in a calculation-based study, we demonstrated the stress-reducing effects of the new load distribution influence factor and the influence of the helix angle on the safety against tooth root breakage with respect to the contact ratio. In addition, by simultaneously varying the transmission ratio and the tool tip radius, we reveal the effect on the updated calculation of internal gears with different tooth root geometries.

All in all, the findings of this research allow a detailed insight into which updates enhance the ISO 6336 standard and how they affect and allow more accurate load carrying capacity calculations.

**Acknowledgment.** The findings presented are part of the research project “FVA-Nr. 814 I – Heft 1371 – Normstudie Stirnradtragfähigkeit. Forschungsvereinigung Antriebstechnik e.V., Frankfurt/Main (2020)”. We therefore thank the Forschungsvereinigung Antriebstechnik e.V. (FVA) and partners for funding and valuable support. Moreover, the calculation based on the current ISO 6336:2019 series is user-friendly available in the *FVA-Workbench* for further use and investigation. 

## References

1. ISO 6336-3:2019-11. 2019, "Calculation of load capacity of spur and helical gears - Part 3: Calculation of tooth bending strength," 6336-3.
2. ISO 6336-3:2006-09. 2006, "Calculation of load capacity of spur and helical gears - Part 3: Calculation of tooth bending strength," 6336-3.
3. ISO 6336-1:2019-11. 2019, "Calculation of load capacity of spur and helical gears - Part 1: Basic principles, introduction and general influence factors," 6336-1.
4. ISO 6336-2:2019-11. 2019, "Calculation of load capacity of spur and helical gears - Part 2: Calculation of surface durability (pitting)," 6336-2.
5. ISO 6336-5:2016-08. 2016, "Calculation of load capacity of spur and helical gears - Part 5: Strength and quality of materials," 6336-5.
6. ISO 6336-6:2019-11. 2019, "Calculation of load capacity of spur and helical gears - Part 6: Calculation of service life under variable load," 6336-6.
7. ISO/TS 6336-4:2019-01. 2019, "Calculation of load capacity of spur and helical gears. Calculation of tooth flank fracture load capacity," 6336-4.
8. ISO/TS 6336-20:2017-11. 2017, "Calculation of load capacity of spur and helical gears. Calculation of scuffing load capacity (also applicable to bevel and hypoid gears). Flash temperature method," 6336-20.
9. ISO/TS 6336-21:2017-11. 2017, "Calculation of load capacity of spur and helical gears. Calculation of scuffing load capacity (also applicable to bevel and hypoid gears). Integral temperature method," 6336-21.
10. ISO/TS 6336-22:2018-08. 2018, "Calculation of load capacity of spur and helical gears. Calculation of micropitting load capacity," 6336-22.
11. ISO/TR 6336-30:2017-11. 2017, "Calculation of load capacity of spur and helical gears - Part 30: Calculation examples for the application of ISO 6336 parts 1,2,3,5," 6336-30.
12. ISO/TR 6336-31:2018-09. 2018, "Calculation of load capacity of spur and helical gears - Part 31: Calculation examples of micropitting load capacity," 6336-31.
13. Paucker, T., M. Otto and K. Stahl. 2019, "Determining the load distribution by measuring the tooth root stresses," *Forsch Ingenieurwes*, 83(3), pp.621–626.
14. Paucker T., M. Otto and K. Stahl. 2019, "A precise prediction of the tooth root stresses for involute external gears with any fillet geometry under consideration of the exact meshing condition," *Proceedings of the Institution of Mechanical Engineers, Part C: Journal of Mechanical Engineering Science*, 233(21–22), pp. 7318–7327.
15. Hotait, M., and A. Kahraman. 2008, "Experiments on Root Stresses of Helical Gears with Lead Crown and Misalignments," *Journal of Mechanical Design, Transactions of the ASME*, 130 (7).
16. Otto M., 2009, "Lastverteilung und Zahnradtragfähigkeit von schrägverzahnten Stirnrädern [Load Distribution and Carrying Capacity of Helical Gears]," Ph.D. Thesis, Gear Research Centre (FZG), *Technical University of Munich*, Munich.
17. Höhn B.-R., P. Oster and M. Otto. 2010, Tooth bending strength of Helical Gears, *International Conference on Gears*.
18. Schinagl, S. 2002, "Zahnfußtragfähigkeit schrägverzahnter Stirnräder unter Berücksichtigung der Lastverteilung [Tooth Root Load carrying Capacity of Helical Gears considering Load Distribution]," Ph.D. Thesis, *Gear Research Centre (FZG), Technical University of Munich*, Munich.
19. Slansky, R. 2015, "Experimentelle und theoretische Untersuchungen zur Fußtragfähigkeit der Innenschragverzahnung [Experimental and Theoretical Investigations on the Root Load carrying Capacity of Internal Helical Gears]," Ph.D. Thesis, *Technical University of Dresden*, Dresden.
20. Linke, H. 2010. *Stirnradverzahnung: Berechnung - Werkstoffe - Fertigung [Spur Gearing - Calculation - Materials - Manufacturing]*, 2nd ed., Hanser, München.
21. VDI 2737:2016-12. 2016, "Calculation of the load capacity of the tooth root in internal toothings with the influence of the gear rim," 2737.

**Stefan Sendlbeck, M.Sc.** is currently a Research Associate at the Institute of Machine Elements, the Gear Research Center (FZG) at the Technical University of Munich in Germany. He started his scientific career with a bachelor's and a master's degree in mechanical engineering from the Technical University of Munich including a study abroad at the University of Waterloo in Canada. He joined FZG as a researcher in 2018. Since then, he focused on gear design and calculation methods, gear condition monitoring and prognostics, and the use of machine learning methods in gear technology.



**Dipl.-Ing. Maximilian Fromberger** is with the calculation and software development department of RENK, a Germany-based company manufacturing transmissions for the industrial, energy and marine sectors, among others. Before that, he was research associate at the Gear Research Center (FZG) of the Technical University Munich. FZG's research focuses on experimental and analytical investigations of endurance, tribology, NVH, materials and fatigue life analysis on gears, transmission components and drive systems. FZG is also developing software that many German gear-related companies rely on. Some of these software products solve mechanical problems; others implement standardized (DIN / ISO) calculation rules. Fromberger was software team leader at FZG. His personal research activities aimed at gear condition monitoring.



**Dr.-Ing. Michael Otto** joined the Gear Research Center (FZG) at the Technical University Munich in 2000 as a research assistant and gained his position as head of department in 2006. He holds a Ph.D. in mechanical engineering, topics of his research activities were load distribution and tooth root carrying capacity. Current research activities include gear geometry, tooth contact analysis and gearbox related NVH. Another main topic is deformation and stress analysis of supporting shafts and bearings in the gearbox. He drives the development of various scientific programs that are available for companies that are member of FVA (German Research Association for Gears and Transmissions). He is head of the research group 'Calculation and Verification of Transmission Systems' at FZG, Prof. K. Stahl, TU Munich.



**Prof. Dr.-Ing. Karsten Stahl** is full professor at the Institute for Machine Elements and director of Gear Research Center (FZG) at the Technical University Munich. FZG research focuses on experimental and analytical investigations of endurance, tribology, NVH, materials and fatigue life analysis on gears, transmission components and drive systems. Prof. Stahl is board member of several scientific associations, convener of DIN and ISO working groups, editor of several scientific journals, author of several hundred publications, and president of the International Conference on Gears.



For Related Articles Search

load carrying capacity

at [www.geartechnology.com](http://www.geartechnology.com)